Coupled constitutive equations for assessing Mechanical effects of Internal Swelling Reactions

Bruno D. Regnicoli Benitez, Jean François Seignol, Boumediene Nedjar

16th ICAAR LISBOA 2021
16th International Conference on Alkali Aggregate Reaction in Concrete
Lisboa | LNEC | Portugal | 1-3 June 2021

Coupled constitutive equations for assessing mechanical effects of Internal Swelling Reactions

Bruno D. Regnicoli Benitez [(1)], Jean-François Seignol [(2)], Boumediene Nedjar [(3)]

(1) *University Gustave Eiffel, Marne-la-Vallé, France, bruno.regnicoli@univ-eiffel.fr*

(2) *University Gustave Eiffel, Marne-la-Vallé, France, jean-francois.seignol@univ-eiffel.fr*

(3) *University Gustave Eiffel, Marne-la-Vallé, France, boumediene.nedjar@univ-eiffel.fr*

Abstract

Internal swelling reactions (*ISR*) in concrete can have significant impact on the long-term behaviour of massive concrete structures. This communication presents the foundations of a constitutive model developed within the framework of the finite-element method. In order to reach, in further step, a correct quantification of the visible crack patterns, we first develop a set of evolutive constitutive equations based on Larive's law and taking into account the main couplings that affect ISR in structures: chemical extent, available moisture, past and present temperature, and creep.

First, the aim of this modelling framework is presented by setting the set of constitutive equations and identifying material parameters on the base of observable data. Then we describe the evolution equation governing the chemical expansion. The third part focuses on coupling with various phenomena. Finally, we propose perspectives about material damage and cracking in concrete.

Keywords*: constitutive equations; coupling; numerical model; parameter identification.*

1. SCOPE AND MOTIVATION

The structural behaviour analysis of structures affected by internal swelling reactions (ISR) as well as the prediction of their future behaviour and the assessment to their lifespan requests the use of numerical models. These models need to be precisely fitted to be relevant, which is often difficult to achieve because information about concrete or construction conditions can be scarce or missing in the case of old structures. The only trustable information is often those directly observed *in situ*: crack patterns or physical quantities collected from monitoring systems. This information is essential in the adjustment of the model to each case study conditions and the model should be able to simulate, in the most realistic way possible, the different phenomena involved.

Two kind of ISR pathologies are considered; the Alkali-Silica Reaction (*ASR*), and the Delayed Ettringite Formation (*DEF*). While for the former, the chemical reaction happens between alkalis in the cement paste and the reactive silica aggregates, the latter is caused by the formation of ettringite in concrete when subjected to high temperature during cement hydration, and later exposed on to moisture. In both cases, the hardened concrete expands progressively which can potentially lead to cracking and structural disorders, to mention a few. It is then of major importance to build numerical tools that can simulate these expanding mechanisms and their consequences on the structural serviceability. For both phenomena, it is unanimously admitted that *ISR* develops when concrete is at high humidity above a certain threshold, or in contact with water.

Extensive research has been conducted so far to model the expansions caused by *ASR* [1–5]. Later on, models have been developed for *DEF* as well, see for example [6–8]. From the mathematical point of view, the models are mostly based on phenomenological approaches formulated in terms of internal variables that can be deployed to feed constitutive relations and evolution laws that must be integrated in a sound way within boundary-value problems that, in a last step, must be solved numerically for the response of concrete structures. This constitutes a good compromise between efficiency and representativity of the complex concrete behaviour.

The *ISR* expansion is in general characterized by two important factors: amplitude, and kinetics. Both are in turn dependent on the humidity level, and on temperature. Hence, by nature, the complete problem at hand is a coupled one thermo-hydro-mechanics. Moreover, other phenomena must be accounted for, e.g., creep, damage, plasticity. In this contribution, details on the creep modelling are given through viscoelastic strain-like internal variables. The plasticity formulation is nowadays classical and is not described for the sake of clarity.

2. GENERAL FRAMEWORK FOR CONSTITUTIVE EQUATION

2.1 Kinematics

Within the continuum, the kinematical choice made in such developments is based on the additive split of the total strain tensor $\boldsymbol{\varepsilon}$ into an elastic part $\boldsymbol{\varepsilon}^{(E)}$ and complementary parts, each one corresponding to a specific phenomenon. we assume that the total strain is the sum:

$$\boldsymbol{\varepsilon} = \boldsymbol{\varepsilon}^{(E)} + \boldsymbol{\varepsilon}^{(T)} + \boldsymbol{\varepsilon}^{(H)} + \boldsymbol{\varepsilon}^{(\chi)} + \boldsymbol{\varepsilon}^{(C)} + \boldsymbol{\varepsilon}^{(P)} \qquad (1)$$

where $\boldsymbol{\varepsilon}^{(T)}$ and $\boldsymbol{\varepsilon}^{(H)}$ are respectively the temperature-induced strain and the hygric-induced strain, $\boldsymbol{\varepsilon}^{(\chi)}$ is the free chemical strain, $\boldsymbol{\varepsilon}^{(C)}$ is the basic creep strain and $\boldsymbol{\varepsilon}^{(P)}$ is the plastic strain.

If θ_0 is defined as the reference temperature and θ as an arbitrary temperature, the thermal strains caused by a change in temperature of an unconstrained isotropic volume are given by:

$$\boldsymbol{\varepsilon}^{(T)} = k_T\,(\theta - \theta_0)\mathbf{1} \qquad (2)$$

where k_T is the coefficient of thermal expansion. Here and in all what follows, $\mathbf{1}$ denotes the second-order identity tensor. Following the same logic, the volumetric strain due to a change in the degree of saturation $\boldsymbol{\varepsilon}^{(H)}$ is given by:

$$\boldsymbol{\varepsilon}^{(H)} = k_S\,(S_R - S_{R,0})\mathbf{1} \qquad (3)$$

with $S_{R,0}$ is the reference degree of saturation, S_R is an arbitrary value of the degree of saturation and k_S is the linear coefficient of hygric expansion. The concrete shrinkage/swelling can easily be expressed in terms of relative humidity too, rather than in terms of degree of saturation.

More complex relationships can be found in the literature for the drying of concrete and it is well known that k_S depends on the relative humidity since the physical mechanisms causing shrinkage change as the humidity decreases. Furthermore, a constant value of k_T neglects its dependence on both temperature and relative humidity. However, a linear relationship between relative humidity and drying shrinkage is a justified approximation in the case of humidity ranging from 50 % to 100 %. Similarly, a constant value for k_T is a well-established approximation when analyzing concrete on a large scale.

Eventually, the free volumetric ASR strain is given by:

$$\boldsymbol{\varepsilon}^{(\chi)} = \varepsilon^{\chi}\,\mathbf{1} \qquad (4)$$

with $\varepsilon^{\chi} = \varepsilon^{\chi}(t,\theta)$ is the free chemical expansion.

2.2 Chemical kinetics

The macroscopic phenomena of *ASR* are modelled within the framework of the porous continua theory, extended to reactive partially saturated porous media [9]. Then, in order to take into account the diffusion conditions as the alkaline reaction develops, as well as accurately representing the sigmoidal chemical expansion-time curve, the model was calibrated on the basis of the extensive and rigorous experimental campaign published in [1].

It follows that the *ASR* strain-induced can be represented as:

$$\varepsilon^{\chi} = \varepsilon_{\infty}\,\frac{1 - exp\,(-\dfrac{t}{\tau_C})}{1 + exp\,(-\dfrac{t+\tau_L}{\tau_C})}\;; \qquad (5)$$

From Equation (5) the chemical expansion can be represented through three parameters, namely, ε_{∞} which is the asymptotic volumetric expansion strain in the stress-free experiment, together with the

characteristic time τ_C and the latency time τ_L of *ASR* swelling.

The previous formulation may also be extended to the case of structures affected by Delayed Ettringite Formation – *DEF*, see for instance [7, 8]. However, the difference lays in the asymptotic volumetric expansion strain; in case of *ASR* ε_∞ is a constant parameter, deduced from experimental tests and depends on the type of concrete, in case of *DEF* $\varepsilon_\infty \equiv \varepsilon_\infty(\boldsymbol{x})$ is a field variable that depends on the thermal history.

In order to take into account this strong dependance the following model, based on experimental work by [10], has been proposed in [6, 7]:

$$\varepsilon_\infty = \alpha \int_0^{t_m} \begin{cases} 0 & if\ \theta \le \theta_{DEF} \\ e^{\left[\frac{E_a^{DEF}}{R}\frac{1}{\theta-\theta_{DEF}}\right]} & if\ \theta > \theta_{DEF} \end{cases} dt \qquad (6)$$

with α is a parameter which accounts for material properties influencing swelling development (cement, aggregates ...), θ_{DEF} is the temperature threshold above which *DEF* occurs, E_a^{DEF} is the activation energy, R is the universal gas constant and t_m is the maturation time.

An alternative formulation can be found in [11, 12]. In any case, during the mechanical analysis, the field $\varepsilon_\infty(\boldsymbol{x})$ is known, which plays a key role in the design of the algorithm.

In the case of constant or monotonically increasing temperature and humidity chemical strain can be expressed by Equation (5). In the case of variable temperature and humidity, characterised even by decreasing functions, the expansion should take into account its irreversibility during time. Within the continuum thermodynamic framework, developing the formulations presented in [1, 2], it can be deduced that the swelling evolution equation can be expressed as follows:

$$\left[\tau_C\ \varepsilon_\infty\left(1+e^{\frac{\tau_L}{\tau_C}}\right)\right]\dot{\varepsilon}^\chi + \left(e^{\frac{\tau_L}{\tau_C}}\right)\varepsilon^{\chi 2} + \left[\varepsilon_\infty\left(1-e^{\frac{\tau_L}{\tau_C}}\right)\right]\varepsilon^\chi = {\varepsilon_\infty}^2. \qquad (7)$$

2.2.1 Temperature dependance

In endothermic reactions, an increase in temperature normally increases the speed of reaction since the energy added to the system allows an easiest combination of reactive ions. This physical result is reinforced, for alkaline reactions, by the way in which accelerated testing is carried out, i.e., high storage temperatures are used in order to accelerate the development of chemical reactions over a period of months, rather than years, time typically needed for AAR to develop within the concrete of structures exposed to the natural environment, [4, 13].

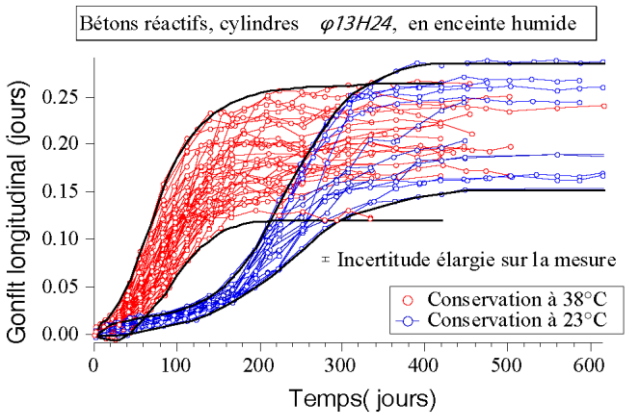

Figure 1: Free expansion from Larive's tests; [1]

The reaction kinetics are highly dependent on temperature, particularly it has been experimentally demonstrated that temperature dependance of time constants τ_C and τ_L matching the Arrhenius equation:

$$\tau_C(\theta) = \tau_C(\theta_0)\, exp[U_C(1/\theta - 1/\theta_0)] \quad (8)$$

$$\tau_L(\theta) = \tau_L(\theta_0)\, exp[U_L(1/\theta - 1/\theta_0)] \quad (9)$$

θ_0 is the reference temperature of expansion test, U_C and U_L are the activation energy constants which cause the thermo-activation of the characteristic and latent times respectively.

2.2.2 Variable moisture conditions

Water plays a dual role in the development of *ASR*: on the one hand, it acts as a carrier for the alkali and hydroxyl ions, allowing the reaction to progress; on the other hand, it is absorbed by the alkali-silica gel which swells, generating the pressure required to crack the concrete [14].

It is widely recognised that below a threshold value of relative humidity (RH = 80-85 %) *ASR* does not occur, [1, 15], and that above this value the expansion increases exponentially, Figure 2.

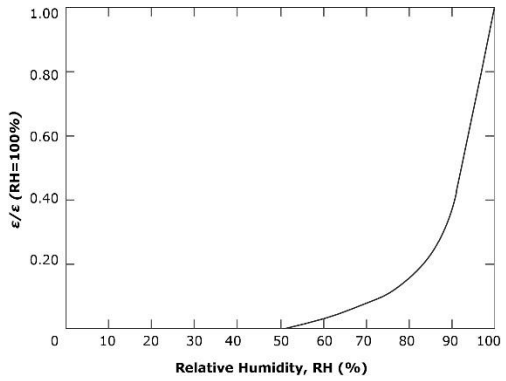

Figure 2 Influence of environmental conditions on chemical expansion: Effect of relative humidity, [16].

Experimental concrete affected by *ASR* also shows a significant dependence between free expansion and variable moisture conditions, [17–21].

In order to simulate the dependence of *ASR* on humidity, and more generally on environmental conditions, mathematical models have been proposed in literature, which take into account the humidity either by reduction functions, [22], or altering the kinetic laws, [20, 21, 23].

Within this framework, an alternative model able to take into account variable humidity conditions is proposed.

In order to capture the moisture effect on the chemical evolution, we use the concept of effective time t_{eff}, introduced in [24, 25], such as:

$$\dot{t}_{eff} = \dot{t}_{eff}(S_R, t) \quad \in [0,1] \quad (10)$$

Now, if $S_{R,\mathrm{thrs}}$ denotes the degree of saturation for which the reaction occurs, we have that:

$$\begin{cases} \varepsilon^{\chi} = 0 & if\ S_R < S_{R,thrs} \\ \dot{\varepsilon}^{\chi} > 0 & if\ S_R \geq S_{R,thrs} \end{cases} \quad (11)$$

Where $\dot{\varepsilon}^{\chi}$ is the chemical strain due to *ASR*, and in the case of constant or monotonically increasing temperature and humidity can be expressed by Equation (5).

The following is a possible option for embedding humidity dependence in chemical evolution equation:

$$t_{eff} = \int_0^t \left(\frac{\langle S_R - S_{R,thrs} \rangle_+}{1 - S_{R,thrs}} \right)^m dt \quad (12)$$

where m is a parameter that depends on the degree of saturation and $\langle\ \ \rangle_+$ denotes the positive part. Furthermore, and besides on the above features, if the final expansion amplitude depends on the level of saturation too, a possible choice to link could be:

$$\varepsilon_\infty(S_R) = \varepsilon_\infty\left(S_{R,1.0}\right)\cdot\left(\frac{\langle S_R - S_{R,thrs}\rangle_+}{1 - S_{R,thrs}}\right)^{m_\infty} \tag{13}$$

where m_∞ is a material parameter that can be identified from free expansion tests carried out at different degree of saturation.

2.3 Visco-elastic behaviour

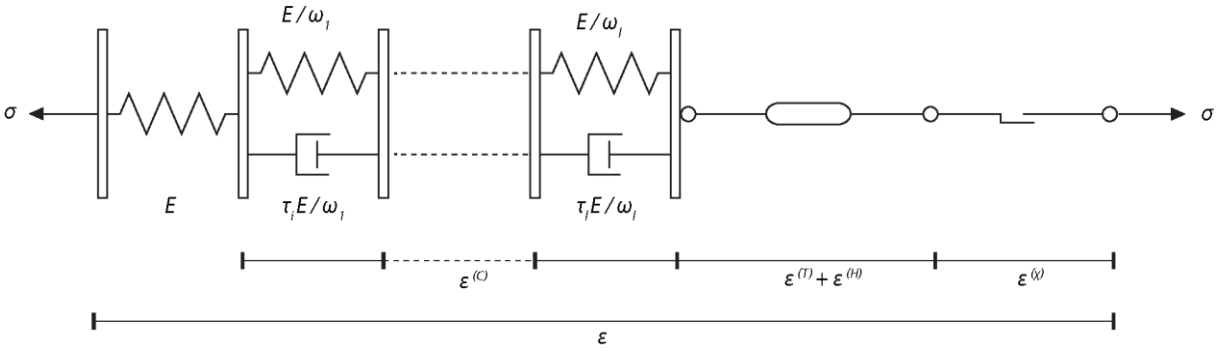

Figure 3 One-dimensional viscoelastic rheological model.

In this framework, creep strain $\varepsilon_{ij}^{(C)}$ is treated as an internal variable, and can be composed of as many contributions as necessary as follows:

$$\boldsymbol{\varepsilon}^{(C)} = \sum_{i=1}^{l} \boldsymbol{\varepsilon}_i^{(C)} \tag{14}$$

Where the $i = 1, \dots l$ hidden variables $\boldsymbol{\varepsilon}_i^{(C)}$ characterize viscoelastic processes with corresponding relaxation times $\tau_i \in [0, +\infty[,\ i = 1, \dots l$. The way all these internal variables evolve is motivated by the generalized Kelvin-Voigt rheological model, Figure 3. In this case, the complementary evolution equations that govern the creep strain components are given by, (for further information see [26]),

$$\dot{\varepsilon}_i^{(C)} + \frac{1+\omega_i}{\tau_i}\,\mathbb{N} : \varepsilon_i^{(C)} + \frac{\omega_i}{\tau_i}\sum_{j=1,\ j\neq i}^{l} \mathbb{N}: \varepsilon_j^{(C)} = \frac{\omega_i}{\tau_i}\,\mathbb{N} : (\varepsilon - \varepsilon^{(T)} - \varepsilon^{(H)} - \varepsilon^{(\chi)}), \qquad i = 1, \dots l \tag{15}$$

where $\omega_i, i = 1, \dots l$ are material parameters. Here $\mathbb{N}$ is the fourth-order tensor which depends solely on the Poisson's ratio ν. In Voigt engineering notation, it is given by:

$$\mathbb{N} = \frac{1}{(1+\nu)(1-2\nu)}\begin{bmatrix} 1-\nu & \nu & \nu & & & \\ \nu & 1-\nu & \nu & & & \\ \nu & \nu & 1-\nu & & & \\ & & & 1-2\nu & & \\ & & & & 1-2\nu & \\ & & & & & 1-2\nu \end{bmatrix} \tag{16}$$

2.4 Constitutive equations and mechanical equilibrium

In the case of a linear elastic relationship for reversible material behaviour, the constitutive relationship can be expressed as follows:

$$\boldsymbol{\sigma} = \mathbf{C} : (\boldsymbol{\varepsilon} - \boldsymbol{\varepsilon}^{(T)} - \boldsymbol{\varepsilon}^{(H)} - \boldsymbol{\varepsilon}^{(\chi)} - \boldsymbol{\varepsilon}^{(C)} - \boldsymbol{\varepsilon}^{(P)}) \tag{17}$$

where $\boldsymbol{\sigma}$ is the stress tensor, $\mathbf{C}$ is the fourth-order elasticity tensor within which a damage mechanism can be introduced as:

$$\mathbf{C} = (1 - d_\chi)\mathbf{C}_0 \tag{18}$$

where $\mathbf{C}_0$ is the elastic modulus for the undamaged concrete and d_χ is a damage variable in the sense of continuum damage mechanics. Indeed, the latter can be related to the chemical expansion explicitly as a function of the quantity $\varepsilon^{(\chi)}$ as follows [7]:

$$d_\chi = 1 - exp\left[-\beta \left\langle \varepsilon^{(\chi)} - \varepsilon_{thrs} \right\rangle_+\right] \tag{19}$$

where $\varepsilon_{thrs}$is the strain-like chemical damage threshold, and $\beta \geq 0$ is a parameter that determines chemical damage occurrence, i.e. for $\beta = 0$ no swelling damage occurs.

2.5 Outlines of the F.E. approximation

2.5.1 Variational formulation

If we consider the weak form of mechanical equilibrium, without taking into account the effects of creep or plasticity, then we will have at the actual time t_{n+1}:

$$\int_{\boldsymbol{B}} \nabla^s \, \delta\boldsymbol{u} : \boldsymbol{C}_{n+1} : \nabla^s \boldsymbol{u}_{n+1} dV = G^{ext}_{n+1}(\delta\boldsymbol{u}) + \int_{\boldsymbol{B}} \nabla^s \, \delta\boldsymbol{u} : \boldsymbol{C}_{n+1} : (\boldsymbol{\varepsilon}^T_{n+1} + \boldsymbol{\varepsilon}^H_{n+1} + \boldsymbol{\varepsilon}^\chi_{n+1}) dV \tag{20}$$

Which must hold for any variation of displacements $\delta\boldsymbol{u}$, and where ∇^s is the symmetric gradient operator. Here G^{ext}_{n+1} is a shorthand notation for the virtual work of the external loads embedding both of the volumetric forces in the body $\boldsymbol{B}$ and traction forces on part of its boundary $\delta_t\boldsymbol{B} \subset \delta\boldsymbol{B}$ applied at time t_{n+1}. Equation (20) is to be solved for the actual displacement field $\boldsymbol{u}_{n+1}$.

The evaluation of the swelling strain $\boldsymbol{\varepsilon}^\chi_{n+1}$ in Equation (20) is carried out through the concept of effective time t^{eff}_{n+1}, which is updated locally at each time step as:

$$t^{eff}_{n+1} = t^{eff}_n + \left(\frac{\langle S_{R,n+1} - S_{R,thrs}\rangle_+}{1 - S_{R,thrs}}\right)^{m_{n+1}} \Delta t \tag{21}$$

Where $\Delta t = t_{n+1} - t_n$ is the real time increment, and m_{n+1} is evaluated at the saturation degree value $S_{R,n+1}$. Consequently, the effective time is treated as an internal field variable ; $t^{eff} = t^{eff}(\boldsymbol{x}, t)$, i.e. within the finite element method the storage is performed at the Gauss points level.

2.5.2 Iterative resolution procedure

In order to extend the use of Equation (20) to non-linear phenomena, such as creep, plastic behaviour, damage mechanics, among others, its resolution is based on an iterative resolution. Hence, assuming a known state $\boldsymbol{u}_{n+1}$ at time t_n, one then solves iteratively the following linearized form for the increment $\Delta\boldsymbol{u}$ of the displacement field:

$$\int_{\boldsymbol{B}} \nabla^s \, \delta\boldsymbol{u} : \widetilde{\boldsymbol{C}}_{n+1} : \nabla^s(\Delta\boldsymbol{u}) dV = G^{ext}_{n+1}(\delta\boldsymbol{u}) - \int_{\boldsymbol{B}} \nabla^s \, \delta\boldsymbol{u} : \boldsymbol{\sigma}^{(i)}_{n+1} \, dV \tag{22}$$

Where, initially for $i = 0$, $\boldsymbol{\sigma}^{(0)}_{n+1} = \boldsymbol{\sigma}_n$. The right-hand side in Equation (22) constitutes the residual of the mechanical balance that is used to test the convergence of the iterative process, and $\widetilde{\boldsymbol{C}}_{n+1}$ is the tangent modulus, whether algorithmic or continuous, computed as:

$$\widetilde{\boldsymbol{C}}_{n+1} = \frac{\boldsymbol{\sigma}^{(i)}_{n+1}}{\partial\boldsymbol{\varepsilon}} \tag{23}$$

Equation (22) is solved together with the appended local evolution equations to update the set of internal variables, i.e. plasticity and/or creep and/or damage. At the end of each global iteration, the displacement field is updated as:

$$\boldsymbol{u}^{(i+1)}_{n+1} = \boldsymbol{u}^{(i)}_{n+1} + \Delta\boldsymbol{u} \tag{24}$$

3. NUMERICAL EXAMPLES

In this section, two numerical examples are presented within the framework of the finite element method. The first one shows the coupling between creep and expansion of a concrete sample, while the second one shows the structural effects of internal reinforcement.

3.1 Basic creep coupled to ISR

It is well known that creep plays a dominant role in the long terms response of concrete structures subjected to constant loads. It is suspected that under swelling due to chemical reaction, the coupling with creep can be more evident. In this first example, we consider cylindrical samples submitted to two levels of axial compressive stress, with uniform relative humidity; one under the swelling threshold where only basic creep takes place, and one at complete saturation where *ISR* is full evolving. More precisely, the following four computations are considered:

(i) Axial compressive stress at $10\ MPa$, with and without *ISR*;
(ii) Axial compressive stress at $20\ MPa$, with and without *ISR*.

For the concrete, we use $E = 20.5\ GPa$ for the Young's modulus, and $\nu = 0.2$ for the Poisson's ratio. For the chemical expansion we choose the parameters:

$$\varepsilon_\infty = 0.4\%,\ \tau_C = 70\ days, \text{ and } \tau_L = 0,$$

And for the basic creep, we use only one mechanism with parameters: $\omega_1 = 1.5$ and $\tau_1 = 150\ days$.

Figure 4 shows the four curves. One can see that, from these computations, the expansion due to *ISR* shows a decrease due to the compressive stress.

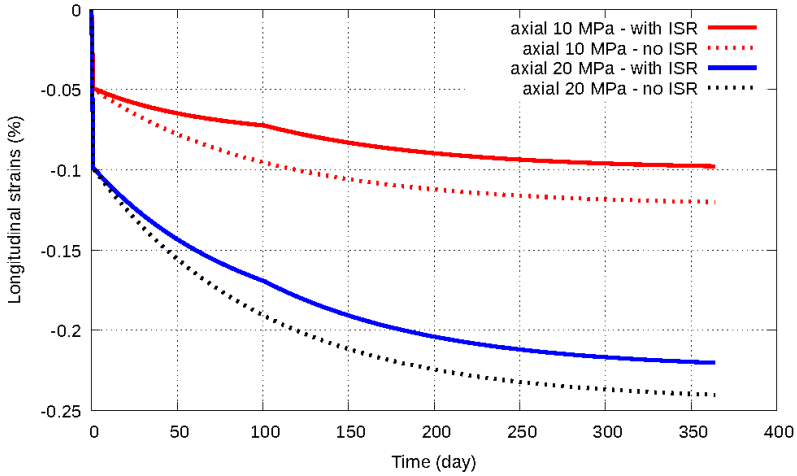

Figure 4 Creep simulations: longitudinal strain evolution for the different compression levels.

3.2 Effect of internal reinforcement

This second example is inspired by a JCI-benchmark example carried out on alkali-aggregate expansion experiments, see for example [27]. Here cylindrical specimens have been considered instead of prismatic ones. They have been constrained uniaxially as shown in Figure 5. Rigid plates on the samples' ends are linked by a steel rebar. Three cases are considered in this set of examples:

(i) a rebar of diameter 6 mm that corresponds to a reinforcement ratio of 0.22%;
(ii) a rebar of diameter 12 mm that corresponds to a reinforcement ratio of 0.88%;
(iii) a rebar of diameter 18 mm that corresponds to a reinforcement ratio of 1.99%.

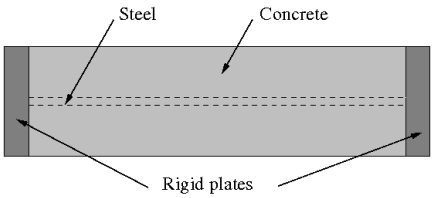

Figure 5 Expansion specimen with a steel rebar

For the sound concrete, we use $E = 25\,GPa$ for the Young's modulus, and $\nu = 0.2$ for the Poisson's ratio. For the chemical expansion we choose the parameters:

$$\varepsilon_\infty = 0.7\%,\ \tau_C = 40\,days, \text{ and } \tau_L = 0.$$

Under fully saturated hydric conditions, the concrete "free" expansion is shown in Figure 5, red curve. Notice that as constant thermo-hydric conditions are considered in all that follows, there is no need to specify the values of the parameters k_T and k_S for the thermo-hydric strains.

For the steel rebars, we consider an elastic-perfectly plastic constitutive relation with the von Mises yield criterion. The parameters we choose are:

$$E_S = 210\,GPa,\ \nu_s = 0.2, \text{ and yield stress } \sigma_y = 550\,MPa.$$

The problem has been discretized by using an axisymmetric analysis. Figure 6 shows the evolution of the mean longitudinal strain within the concrete specimens for the above mentioned reinforcement ratios and for a unreinforced concrete specimen (red curve), which correspond to a free-expansion.

For the measured longitudinal strains on reinforced and unreinforced specimens, it has been observed that for the highest reinforcement ratio (here with 1.99%, green curve), the elastic strain limit is not reached within the steel rebar. This is not the case for the remaining reinforcement ratios (0.88% and 0.22% ratios, respectively, blue and black curves), where, according to the stress-strain relationship considered, the reinforcements are such that plastic yield stress has been reached in the rebars.

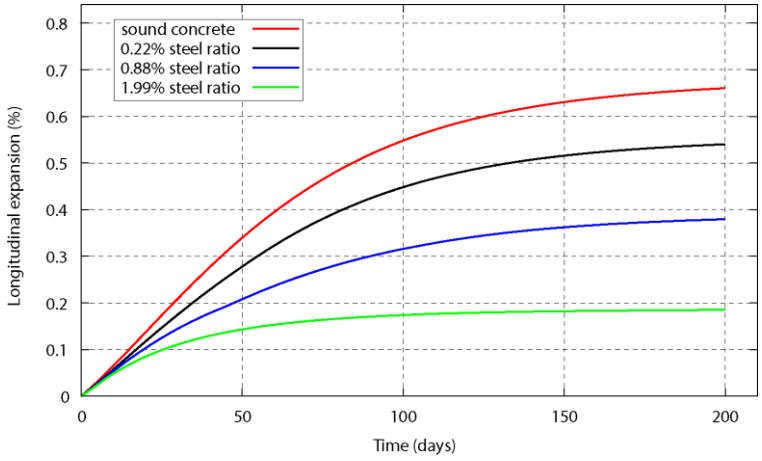

Figure 6 Longitudinal expansions evolutions for the different steel ratios.

4. CONCLUSION AND PERSPECTIVES

In the present study, a numerical tool has been developed for modelling ISR under variable environmental conditions.

The swelling development has been formulated within the framework of continuous thermodynamics, which also allows irreversible phenomena to be taken into account. Both temperature and relative humidity play a key role in the development of ISR. In the present model, the concept of "effective time" has been introduced into the swelling kinetic law to account for variable humidity, instead, the

dependence on past and present temperature are included within the two time constants of the reaction, the characteristic and latency time.

In order to perform efficient structural calculations, the model covers different mechanisms observable in concrete including creep, drying shrinkage, thermal dilatation and plastic behaviour. Viscous phenomena have been modelled through a generalised Kelvin-Voigt rheological model to formulate the whole behaviour. Long-term and short-term relaxation processes can be integrated into the model by means of all necessary viscoelastic processes.

The effectiveness of this model has been demonstrated in two numerical examples. The first focuses on the analysis of coupling between creep and ISR, while the second example investigates the swelling strain due to ASR/DEF over time in reinforced concrete specimens.

The numerical results highlighted the relevance of taking into account the interaction between these phenomena when formulating a numerical model to predict the evolution of strain swelling.

Future work will focus on establishing a relationship between cracking on the facing and the internal state of the structure. This would open the door to a field in which engineering will allow for better analysis of the structural behaviour of existing structures such as bridges, dams, nuclear power plants, to name a few.

5. REFERENCES

1. Larive C (1997) Apports combinés de l'expérimentation et de la modélisation à la compréhension de l'alcali-réaction et de ses effets mécaniques. Université Paris Est
2. Li K, Ulm F-J, Coussy O, et al (2000) Chemoelastic modelling of ASR in concrete. In: 11th International conference on alkali aggregate reaction. Québec, pp 989–998
3. Ulm F-J, Coussy O, Li K, Larive C (2000) Thermo-chemo-mechanics of ASR expansion in concrete structures. J Eng Mech © ASCE 233–242
4. LCPC (1997) Alcali-réaction du béton Essai d'expansion résiduelle sur béton durci, Projet de. Techniques et méthodes des Laboratoires des Ponts et Chaussées
5. Multon S, Seignol JF, Toutlemonde F (2005) Structural behavior of concrete beams affected by alkali-silica reaction. ACI Mater. J. 102:67–76
6. Baghdadi N, Seignol J, Toutlemonde F (2007) Modélisation du couplage chimico-mécanique pour calculer une structure en béton atteinte de réaction sulfatique interne. In: 18ème Congrès Français de Mécanique, 18ème Congrès Français de Mécanique Grenoble. Grenoble, pp 27–31
7. Seignol J-F, Baghdadi N, Toutlemonde F (2009) A macroscopic chemo-mechanical model aimed at re-assessment of delayed-ettringite-formation affected concrete structures. In: The first international conference on computational Technologies in Concrete Structures (CTCS'09). Jeju, Corea
8. Baghdadi N (2008) Modélisation du couplage chimico-mécanique d'un béton atteint d'une réaction sulfatique interne. Ecole Nationale des Ponts et Chaussées
9. Coussy O (1996) Mechanics of porous continua. IEEE Electr. Insul. Mag. 12:49
10. Brunetaud X (2005) Etude de l'influence de différents paramètres et de leurs interactions sur la cinétique et l'amplitude de la réaction sulfatique interne au béton. Ecole centrale de Paris
11. Martin R-P (2010) Analyse sur structures modèles des effets mécaniques de la réaction sulfatique interne du béton. Université Paris Est
12. Martin R-P, Bazin C, Billo J, et al (2012) Experimental Evidence for Understanding Def Sensitivity To Early-Age Thermal History. CONCRACK 3 – RILEM-JCI Int Work Crack Control Mass Concr Relat Issues Concern Early-Age Concr Struct 1–10
13. LCPC (2009) Réaction sulfatique interne au béton - Essai d'éxpansion résiduelle sur carotte de béton extraite de l'ouvrage, Les collec. Paris
14. Sims I, Poole AB (2017) Alkali-aggregate reaction in concrete: A world review. Taylor and Francis
15. Larive C, Laplaud A, Coussy O (2000) The Role of Water in Alkali-Silica Reaction. In: International conference, Alkali-aggregate reaction in concrete; 2000. ICON/CANMET, Quebec City, Canada, pp 61–70
16. Poole AB (1992) The alkali-silica reaction in concrete. Blackie u.a., London u.a.

17. Multon S, Seignol JF, Toutlemonde F (2005) Structural behavior of concrete beams affected by alkali-silica reaction. ACI Mater J 102:67–76. https://doi.org/10.14359/14299
18. Multon S, Seignol JF, Toutlemonde F (2006) Concrete beams submitted to various moisture environments. Struct Eng Mech 22:71–83. https://doi.org/10.12989/sem.2006.22.1.071
19. Multon S, Toutlemonde F (2010) Effect of moisture conditions and transfers on alkali silica reaction damaged structures. Cem Concr Res 40:924–934. https://doi.org/10.1016/j.cemconres.2010.01.011
20. Poyet S (2003) Etude de la degradation des ouvrages en beton atteints par la reaction alcali-silice - approche experimentale et modelisation numerique des degradations dans un environnement hydro-chemo-mecanique variable. Université de Marne-la-vallé
21. Poyet S, Sellier A, Capra B, et al (2006) Influence of Water on Alkali-Silica Reaction: Experimental Study and Numerical Simulations. J Mater Civ Eng 18:588–596. https://doi.org/10.1061/(asce)0899-1561(2006)18:4(588)
22. Capra B, Bournazel JP (1998) Modeling of induced mechanical effects of alkali-aggregate reactions. Cem Concr Res 28:251–260. https://doi.org/10.1016/S0008-8846(97)00261-5
23. Li K (2002) Modélisation chimico-mécanique du comportement des béetons affectés par la réeaction d'alcali-silice et expertise numéerique des ouvrages d'art déegradés. PhD Thesis - ENPC 1–219
24. Nedjar B, Rospars C, Martin RP, Toutlemonde F (2021) Benchmark Study Results: IFSTTAR. In: RILEM Technical Committee 259-ISR, Diagnosis & Prognosis of AAR Affected Structures, Ed. V. Sao. Springer Science+Business Media B.V., pp 427–437
25. Malbois M, Nedjar B, Lavaud S, et al (2019) On DEF expansion modelling in concrete structures under variable hydric conditions. Constr Build Mater 207:396–402. https://doi.org/10.1016/j.conbuildmat.2019.02.142
26. Nedjar B, Le Roy R (2013) An approach to the modeling of viscoelastic damage. Application to the long-term creep of gypsum rock materials. Int J Numer Anal Methods Geomech 37:1066–1078. https://doi.org/10.1002/nag.1138
27. Ishikawa TT and Y (2017) Chemical Expansion Effect in Concrete and its Numerical Simulation Based on the Mechanical Energy Conservation Hypothesis. In: JCI-RILEM International Workshop on Control of Mass Concrete and Related Issues Early Age Cracking of Structures (CONCRACK). TOKYO, Japan, pp 161–174